Al-Mukhtar Journal of Sciences 37 (2): 150-161, 2022
ISSN: online 2617-2186 print 2617-2178
Journal Homepage https://omu.edu.ly/journals/index.php/mjsc/index

Identification of Potential Natural Bioactive Compounds from *Glycyrrhiza glabra* as Sars-CoV-2 Main Protease (MPRO) Inhibitors: *In-Silico* Approach

Ashraf Ahmed Ali Abdusalam[1]*, Gazala Mohamed Ben-Hander[2]

[1] *Department of Pharmaceutical Chemistry, Faculty of Health Sciences, Sirte University, Libya*
[2] *Department of Chemistry, Faculty of Sciences, Sirte University, Libya*

Received: 20 March 2022./ Accepted: 04 June 2022
Doi: https://doi.org/10.54172/mjsc.v37i2.679

Abstract: The SARS-CoV-2 virus caused the COVID-19 pandemic declared in early 2020, generating a global health emergency. So far, no approved drugs or vaccines are available. Therefore, there is an urgent need to explore and develop effective new therapeutics against SARS-CoV-2. In addition, the main protease (Mpro) of the SARS-CoV-2 virus is considered essential in the virus replication propagation and considered a drug discovery target. Consequently, plant-derived compounds are an important and valuable source for novel drugs. This study reports molecular docking-based virtual screening (VS) of 20 compounds identified from Glycyrrhiza glabra to search for potent compounds against 3CL proteases (3CLpro). The screening results revealed that the identified compounds Semilicoisoflavone B, Licoflavone B, and Licocoumarin A exhibited low free energy of binding (FEB) values of 10.91, −10.29, and −10.21 kcal/mole for Autodock 4.2 and −9.81, −9.77, and −9.60 kcal/mole, for AutoDockVina, respectively. The obtained results of FEB in this study were better than the coordinated ligand N3, which was -7.4 kcal/mole. The three potential compounds showed different and stable interactions with the essential amino acids, especially the catalytic dyad (Cys145-His41) in the binding pocket of the 3CLpro. Three potential inhibitors were successfully identified from Glycyrrhiza glabra using molecular docking and virtual screening; these compounds obeyed the Lipinski rule of 5 with a little violation and showed low FEB and good interactions with the 3CLpro. These identified compounds may serve as potential leads that help in developing therapeutic agents against the SARS-CoV-2. Further research is recommended (in vitro and in vivo) to verify the above findings.

Keywords: Virtual Screening, Docking, *Glycyrrhiza glabra,* COVID-19, SARS-CoV-2, 3CL protease.

INTRODUCTION

The recent outbreak of severe acute respiratory syndrome (SARS) coronavirus disease-19 (COVID-19) is a novel infectious and highly contagious disease that first appeared in Wuhan, Hubei Province, China, in December, the year 2019 (Phan, 2020; Yang et al., 2020). The virus has spread worldwide, increasing the number of victims and causing significant morbidity and mortality. On March 11, 2020, the World Health Organization (WHO) classified it a pandemic (Asrani et al., 2021; Zehra et al., 2020). SARS-CoV is a novel member of the betacoronavirus genus, which belongs to the Coronaviridae family. It has an enveloped, positive-sense, sin-

***Corresponding author:** Ashraf Ahmed Ali: aalmansory@su.edu.ly , Department of Pharmaceutical Chemistry, Faculty of Health Sciences, Sirte University, Libya.

gle-stranded RNA (Chan et al., 2020; Pal et al., 2020). The viral genomes encode as non-structural proteins (NSPs), which include (3-chymotrypsin-like protease 3CLpro) nsp5, (papain-like protease) nsp3, (helicase) nsp13, and (RNA-dependent RNA polymerase [RdRp]) nsp12, in addition to structural proteins (such as spike glycoprotein and accessory proteins) (Chan et al., 2016; Chan et al., 2020). These two proteases (PLpro and 3CLpro) are involved in the transcription and replication of the virus. However, the 3CLpro mainly has the most important role in virus replication (De Wit et al., 2016).

There is currently no therapeutically licensed inhibitor of the SARS protease, but several are being developed (Stoermer, 2020). In addition, protease inhibitors have been developed for a variety of viruses, including nelfinavir (Gills et al., 2007), amprenavir for HIV (Marcelin et al., 2003), and lopinavir-ritonavir (Sáez-Llorens et al., 2003) for HCV. However, manufacturing those protease inhibitors requires a multistep reaction that is quite costly, and an emergency medicine that is both effective and inexpensive is currently needed. It is well known that several medicinal plants may combat viruses and have active components that produce large quantities of data about their effectiveness. Glycyrrhiza glabra is one of these therapeutic plants, and its active components may have the ability to combat numerous viruses (Pompei et al., 1980). Glycyrrhiza glabra (Gg), often known as 'sweet wood' and 'liquorice', is a member of the Fabaceae family.

It is effective against a variety of RNA viruses, including the influenza A virus, H1N1 virus, H5N1 virus, Rotavirus, Newcastle disease virus, Hepatitis C virus, and severe acute respiratory virus, as well as DNA viruses, including Herpes Simplex virus, Epstein-Barr virus, and Varicella-Zoster virus (Cinatl et al., 2003; Wang et al., 2015). Several potent compounds derived from Gg have been identified as being capable of inhibiting the virus's development. It has been demonstrated in some research studies that Glycerrhizin (Glycyrrhizinate or Glycyrrhizic acid) is effective in inhibiting the binding of viruses to target cells, as well as in controlling viral replication. It has been observed to have considerable antiviral activity (Sharma et al., 2018; Wang et al., 2015).

The application of computational methods in drug discovery has assisted in the acceleration of the discovery and design of new drug candidates while also lowering the overall cost of the process. As a result, virtual screening-based drug discovery has been identified as one of the most effective ways of discovering new drugs.(Zoete et al., 2009). In-silico virtual screening is a searching strategy used to discover novel compounds and chemotypes that can be utilized as alternatives to currently available drugs (Ahmed Ali Abdusalam & Vikneswaran, 2020; Sliwoski et al., 2014). With the help of VS, also known as the step-by-step approach of sequential filters, it is possible to narrow down a large number of compounds to select the most promising lead-like hits that have potential biological activity against a target protein (Jacq et al., 2007; Lavecchia & Di Giovanni, 2013; McInnes, 2007).

In this study, the VS approach was carried out to identify and estimate potential inhibitors against two SARS-CoV-2 3CL proteases obtained from the Allium roseum L plant, followed by molecular docking to discover new inhibitors that may be used in the treatment of coronavirus infections.

MATERIALS AND METHODS

Retrieval and Preparation of Protein Structure*:* The three-dimensional structure of 3CLpro of SARS-CoV-2 in complex with inhibitor N3 was retrieved from the Protein Data Bank (http://www.rcsb.org) (Berman, 2000) (PDB ID: 6LU7), and the structure is shown in Figure 1 (Burley et al., 2017). Autodock Tools (ADT) was used to remove co-factor and unwanted water molecules, add the

polar hydrogen to the protein, compute Gasteiger, and add Kollman charge. Subsequently, the file is saved in the PDBQT format.

Ligand Preparation: The three-dimension structures (3D) of the 20 ligands were obtained from the PubChem site (http://pubchem.ncbi.nlm.nih.gov). The downloaded ligands were in SDF format. BIOVIA Discovery Studio Visualizer 2016 www.accelrys.com was used to convert ligands to PDB, and ligands were converted to PDBQT for VS using raccoon software. Molecular proprieties used for Lipinski's (RO5) (Lipinski, 2004) were evaluated using the online-site Molinspiration https://www.molinspiration.com/cgibin/properties**.**

Virtual Screening: AutodockVina was used to perform an initial virtual screening of 20 bioactive compounds against SARS-CoV-2 3CLpro (PDB ID: 6LU7). The protein file was converted from PDB to PDBQT, and a Config.txt file with all of the information needed for VS with ADT was created; all other options were considered a default.

Moleculaer Docking: Molecular docking is a computational technique for determining the ligand's best shape and orientation when interacting with a receptor (Morris et al., 2009). This research was to take the search one step further by determining the binding affinity of the selected compounds for the target protein. The docking simulation and analysis were carried out using AutoDock 4.2 and AutoDockVina (Trott & Olson, 2010). AutoDock 4.2 was used to find the optimal orientation and interactions between the ligand and bioactive compounds; the grid box parameter was set as 60-60-60 for the x-, y-, and z-axes, respectively, with a spacing of 0.375 Å positioned at the centre of the binding pocket. For each docking experiment, 100 independent runs were performed. For each conformation, the lowest binding energy was chosen.

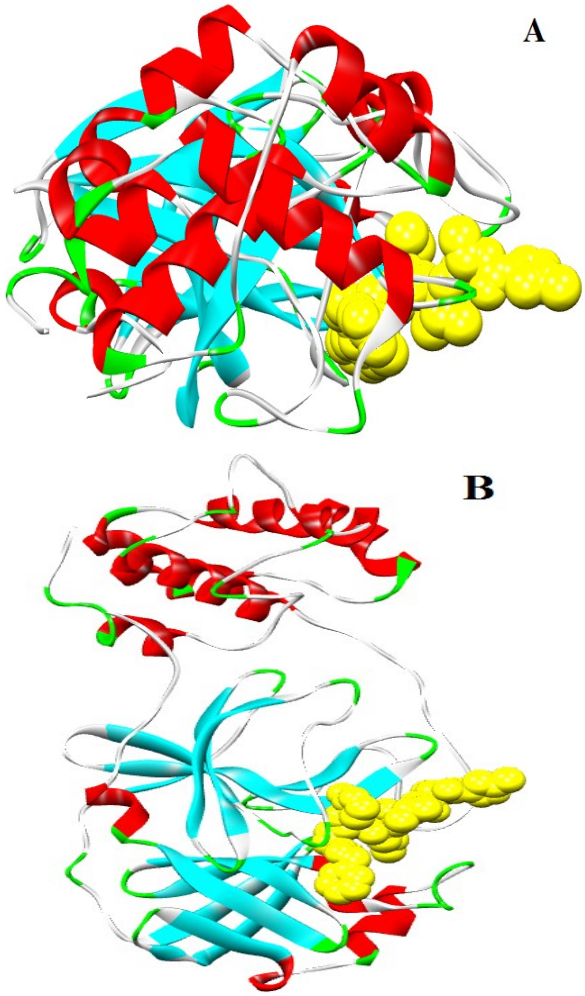

Figure: (1). Diagram representation of the three-dimensional structure 3D of 6LU7 in complex with N3 (yellow color) (A) Orthogonal view (B) Side view.

RESULTS AND DISCUSSION

Validation of The Virtual Screening Protocol: Prior to performing the virtual screening and molecular docking, validation of the docking protocol was evaluated by a re-dock within the acceptable range of the co-crystallized N3 to the target protein's active site (PDB: 6LU7). Here, the N3 pose exhibited the same orientation pattern as the crystallographic pose (RMSD = 0.82 Å, Figure 2, binding affinity −7.2 kcal/mol). Therefore, the results showed that the used protocol was reliable, and the docking software can be trusted and reproduce the expected binding mode of the co-crystallized ligand.

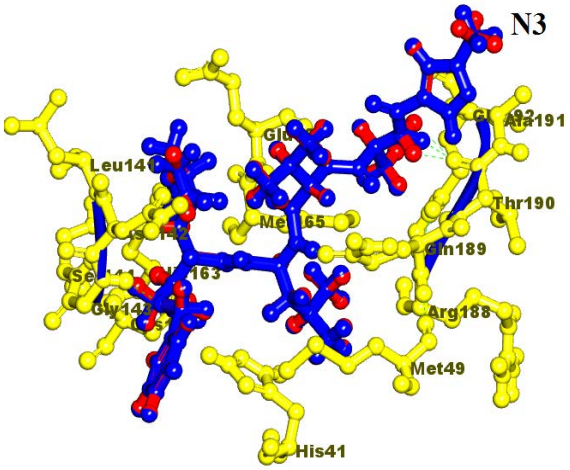

Figure: (2). Superimposition of the docked and crystallographic N3 poses (red and blue), respectively.

Initially, 20 compounds identified from Glycyrrhiza glabra were obtained from the literature (Pastorino et al., 2018). The compounds were virtually screened against the target protein and arranged according to the FEB. The top three compounds that exhibited the lowest energy of binding were chosen. Then, the Lipinski Role of five was used based on the molecular properties of the compounds to assess their similarity with approved drugs. The role of the top potential hits compounds is shown in Table 1. This rule is used to determine the drug-likeness properties should be no more than one violation of the following criteria, ALogP < 5, molecular weight < 500, number of HBD < 5, number of HBA < 10, and rotatable bond < 10. As can be seen from Table 1, the three compounds fall within the acceptable range of the Lipinski rule; the Semilicoisoflavone B compound was fully obeying the rule, while the other two compounds, Licoflavone B and Licocoumarin A, violate only one rule, whereas the coordinated ligand N3 violated more than two rules.

Figure 3 depicts the top three bioactive compounds ranked by AutoDockVina scores. These molecules exhibited the lowest FEB among the other compounds in the protein-ligand complex; subsequently, they were applied in the docking calculation. The docking simulation results showed that all the 20 compounds displayed FEB in the range -9.8- to -3.3 kcal/mol. Therefore, the compounds that showed the lowest FEB were considered the best, Table 2.

Therefore, the top 3 ranked compounds were suggested as the most suitable candidates. Semilicoisoflavone B, Licoflavone B, and Licocoumarin A displayed a minimum FEB of -9.8, -9.7, and -9.6 kcal/mol by AutoDockVina and the energy of -10.91,-10.29, and -10.21 kcal/mol by AutoDock 4.2, respectively, Table 3.

Table: (1). Molecular properties of the three 3CL pro inhibitor candidates.

No	Name	Molecular weight(g/mol)	logp	H-bond donors	H-bond acceptors	Rotatable bonds	Lipinski's rule violation	Drug-likeness alert
1	Semilicoisoflavone B	352.34	3.43	3	6	1	0	Accepted
2	Licoflavone B	390.50	6.3	2	4	5	1	Accepted
3	Licocoumarin A	406.47	5.59	3	5	5	1	Accepted
4	N3	680.35	2.32	5	14	18	2	----------

The clustering analysis is considered the best method to determine if the docking simulation effectively searched the available conformation space. Furthermore, pose clustering is a method for identifying possible poses that are different from energy ranking, and it can help decrease the number of strange poses (Forli et al., 2016; Makeneni et al., 2018; Morris et al., 1998).

Table: (2). Free energy of binding for the 20 compounds against COVID-19 3CLpro.

No	Compound Name	Free energy of binding Kcal/mole
1	Semilicoisoflavone B	-9.8
2	Licoflavone B	-9.7
3	Licocoumarin A	-9.6
4	Shinpterocarpin	-8.8
5	Glabridin	-8.8
6	1-Methoxyficifolinol	-8.6
7	enoxolone	-8.5
8	Licopyranocoumarin	-8.1
9	1-Methoxyficifolinol	-8.0
10	enoxolone	-7.8
11	Glisoflavone	-7.7
12	Isoliquiritigenin	-7.5
13	Liquiritigenin	-7.5
14	Isoangustone	-7.4
15	Liquiritin	-7.3
16	Licoarylcoumarin	-7.3
17	Licochalcone a	-7.2
18	Kanzonol R	-7.2
19	Licoriphenone	-7.1
20	Glycyrrhizic acid	-3.3

Table: (3). FEB Binding energy values of the 3 compounds present in Glycyrrhiza glabra.

No	Compound	AutoDock 4.2 (kcal/ mol)	AutoDock-Vina (kcal/mol)
1	SemilicoisoflavoneB	-10.91	-9.8
2	Licoflavone B	-10.29	-9.7
3	Licocoumarin A	-10.21	-9.6

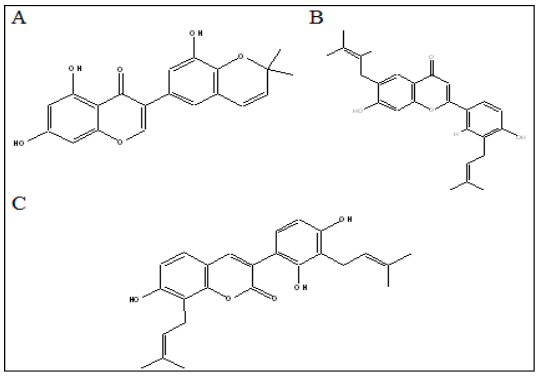

Figure: (1). Structure of the top three 3CL protease inhibitor (A) Semilicoisoflavone B (B) Licoflavone B (C) Licocoumarin A.

The results obtained by AutoDock 4.2 are organized by the FEB and the cluster of solutions that adopt the same pose Table 4 (Smith et al., 2004). The results for compound Semilicoisoflavone B exhibited 58 poses adopted as favourable conformation (this pose is considered the largest cluster out of 100 poses).

Licoflavone B adopted poses 19 times out of 100. Likewise, Licocoumarin A took this pose 46 times. The best docking solution was reported by Autodock (lowest FEB) for each GA run, as well as the cluster rank of the selected docked structure, the docked free energy range of docked structures, and the docked free energy of the selected docked structure Table 4. Only the docking mode that exhibited the lowest FEB was chosen for this cluster. Amino acid residues fully wrapped these molecules at the binding pocket region, as shown in Figure 4.

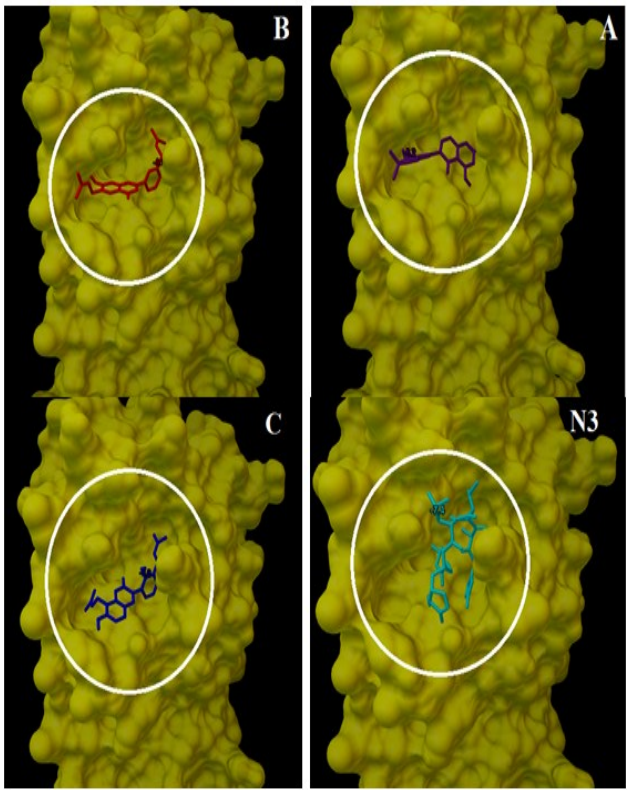

Figure: (4). Enfolding of the three compounds in the binding pocket, (A)Semilicoisoflavone B (B) Licoflavone B and (C) Licocoumarin A.

Table: (4). Docked FEB and relative cluster ranks of the three compounds.

No	compounds	Number of AutoDock clusters a	Cluster rank of selected docked structure	Docked free energy range of docked structures	Docked free energy of selected docked structure
1	Semilicoisoflavone B	58 (100)	4	-10.91 to -8.88	-10.91
2	Licoflavone B	19 (100)	3	-10.29 to -8,21	-10.29
3	Licocoumarin A	46 (100)	2	-10.21to -9.31	-10.21

The docking location of the three compounds was investigated. The interaction analysis results revealed that all compounds occupied the same position in the active pocket with a comparable pattern. Thus, the compounds were covalently bound by the essential amino acid residues of the target protein. The interactions of the docked compounds with the protein were manually examined, and then the location of the compounds in the binding pocket was determined. They showed extensive interactions with the key amino acids residues constructing the binding pocket. The interactions are hydrogen bonds, Van der Waals interaction, Pi-alkyl, Pi-sigma, Pi-cation, Pi-anion, and hydrophobic interaction, as shown in Figure 5.

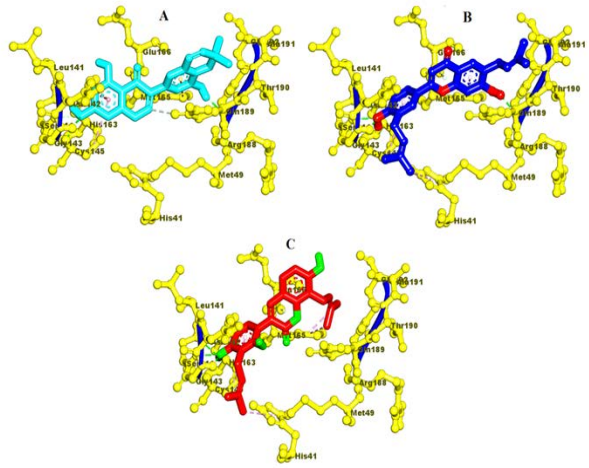

Figure: (5). The 3D structure of the three potential compounds (A) Semilicoisoflavone B (B) Licoflavone B (C) Licocoumarin A

The compound, Semilicoisoflavone B, was found to form five hydrogen bonds, four between amino acids SER144, CYS145, GLY143, LEU141, and oxygen atom O_2, and the fifth H-bond was between ARG188 and the fifth O_2 atom on the compound. The amino acids HIS41, CYS145, and PRO168 showed three Pi-Alkyl bonds between the benzene ring and methyl group, respectively. HIS163 exhibited a Pi-Sulfur bond with a benzene ring on the compounds. Likewise, hydrophobic interactions were displayed with amino acids THR190, PRO168, GLN189, GLU166, ARG188, MET165, ASN142, and HIS41 at the binding pocket. Van der Waals interactions were also noticed between THR190, GLN192, CLU166, and ASN142 and the carbon atoms C-1, C-5, C-11, and the C-14 compound. A carbon-hydrogen bond formed with the amino acid GLN189 and benzene ring (Table 5 and Figure 6).

The Compound Licoflavone B was found to show three hydrogen bonds between amino acids GLY143, ARG188, SER144, and oxygen atom O_2. Amino acid HIS41, CYS145, MET165, and LEU27 formed four Pi-Alkyl bonds with the two benzene rings and two methyl groups. Likewise, a carbon-hydrogen bond formed with amino acid GLU166. In addition, hydrophobic interactions were displayed between amino acids HIS41, CYS145, GLN189, HIS163, LEU144, THR90, AEG188, MET165, and GLU166. The other interaction shown was van der Waals, exhibited between amino acids GLN192, THR190, PRO168, HIS163, LEU141, THR25, ASN142, and carbon atoms C-1, C-2, C-3, C-7, C-13, C-19, C-20, C-23, C-23, and C-25, and different carbon atom on the compound (Table 5 and Figure 6). The compound Licocoumarin A showed three hydrogen bonds, two between amino acids SER144 and oxy-

gen atom O_2, another one with GLY143 and the same oxygen atom. Amino acids HIS41, LEU27, CYS145, LEU167, and MET165 formed six Pi-alkyl bonds, one with a benzene ring and four with methyl groups on the compound. In addition, van der Waals interactions were displayed between amino acids THR29, THR26, ASN142, PRO168, GN192, THR190, GLN189, ARG188, HIS163, LEU141, and carbon atoms C-1, C-2, C-5, C-8, C-15, C-9, C-17, C-19, and C-20 of the compound. The compound formed hydrophobic interactions with amino acids GLN192, THR26, ASN142, LEU27, LEU141, HIS41, HIS163, GLU166, THR190, MET165, GLN189, and ARG188 (Table 5 and Figure 6).

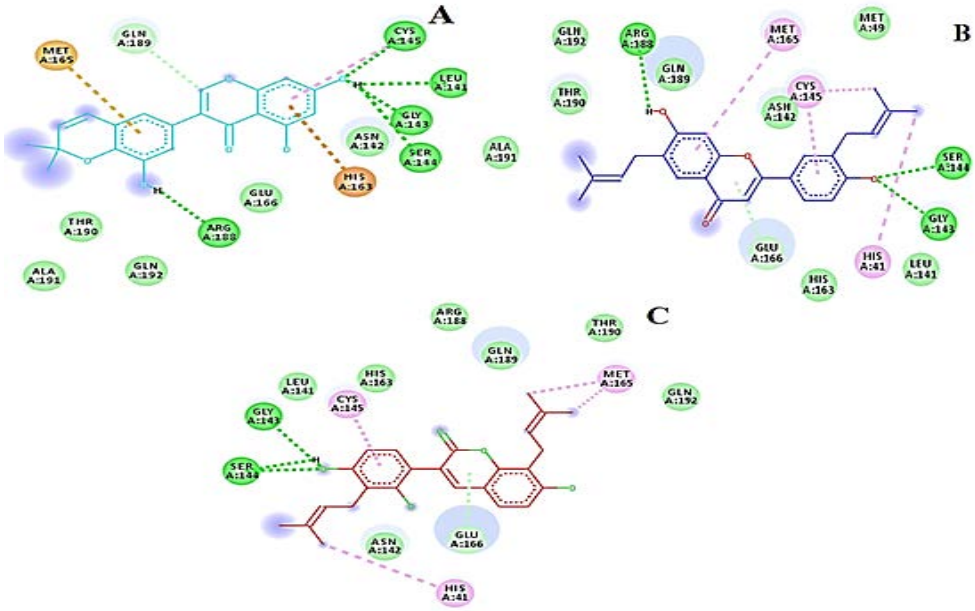

Figure: (6). The 3D structure of the three potential compounds using Discovery studio visualizer (A) Semilicoisoflavone B (B) Licoflavone B (C) Licocoumarin A.

Table: (5). Details of binding interactions of the potential four compounds docked into the active pocket of the COVID-19 3CLprotease.

	Ligands	Residue	Type of interactions
1	Semilicoisoflavone B	CYS145, SER144, GLY143, LEU141, ARG188, THR190, GLN192, CLU166, ASN142, MET165, HIS41, PRO168 GLN189 HIS163 SER144, GLY143,ARG188, GLN192, THR190, PRO168, HIS163, LEU141, THR25, ASN142, HIS41, CYS145, MET165,LEU27 GLU166 CYS145, GLN189, THR90AEG188, MET165, GLU166, LEU144, HIS163, HIS41 SER144, SER144,GLY143 THR29, THR26, ASN142, PRO168, G,N192, THR190, GLN189,ARG188, HIS163, LEU141 HIS41, LEU27, CYS145, LEU167, MET165 LEU27, THR26, ASN142, LEU141, HIS41, HIS163, GLU166, MET165, GLN192, THR190GLN189, ARG188	H-Bond van der Waals Pi-Sulfur Pi-Alkyl Carbon Hydrogen Bond Pi-Cation H-Bond van der Waals Pi-Alkyl Carbon Hydrogen Bond Hydrophobic H-Bond van der Waals Pi-Alkyl Hydrophobic
2	Licoflavone B		
3	Licocoumarin A		

LigPlot (Laskowski & Swindells, 2011) was used to confirm the results of the interactions between the compounds and the target protein; as can be seen in Figure 7, which showed that the compounds occupy the binding pocket and display different interactions such as H-bond, hydrophobic interaction, which indicates the efficiency and effectiveness of these compounds against COVID-19. As mentioned earlier, the hydrogen bond and hydrophobic interactions between the ligands and protein are critical for ligand binding.

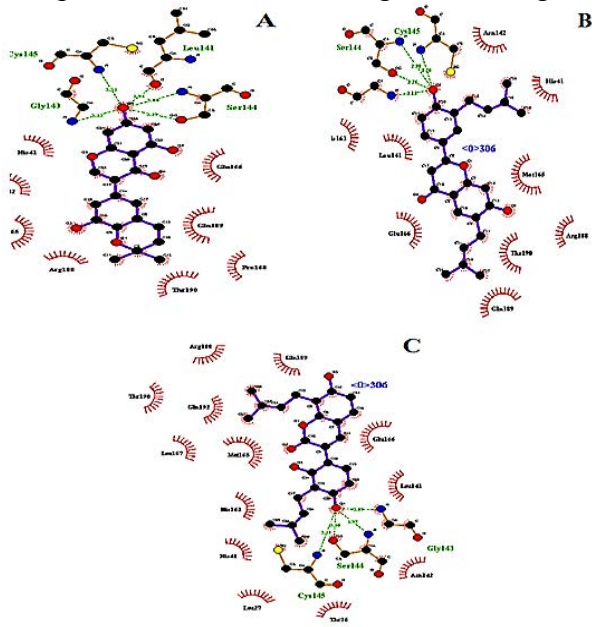

Figure: (7). The 2D structure of the three potential compounds using LigPlot (A) Semilicoisoflavone B (B) Licoflavone B (C) Licocoumarin A.

In this study, in-silico structure-based drug design was employed to apply a logical and inexpensive technique to accelerate the discovery of effective SARS Coronavirus-2 antiviral drugs (Ahmed Ali Abdusalam & Vikneswaran, 2020; Hariyono et al., 2021) The docking results of the three compounds from Glycyrrhiza glabra against the target protein determined minimum FEB, molecular characteristics, binding mode, hydrophobic interactions, and hydrogen-bond between the amino acids residues and compounds in the binding pocket. Therefore, this research involved screening the molecular properties, two docking software (Autodock 4.2 and AutodockVina), hydrogen bonding, and hydrophobic interaction analysis. Even though the use of structural and molecular properties analysis applied in the study was not complicated and easy to use, it helped minimize the costs and the number of docked compounds. In addition, they increased the precision of the virtual screening approach and the consistency of the results of the current study. As long as the catalytic dyad Cys145 and His41 are very important in the covid-19 inhibition, the above finding successfully identified three potential compounds from Glycyrrhiza glabra that displayed good binding interactions and low binding affinity. The three compounds were inhibitors for the catalytic dyad alongside the essential amino acids in the binding pocket. This ability to interact with the essential amino acids in the COVID-19 3CLpro gives additional advantages of inhibiting the virus activity.

CONCLUSION

The current study applied a combination of different molecular modeling techniques, such as two molecular docking approaches, molecular features screening, hydrogen-bond, and hydrophobic interactions analyses, and successfully identified three potential inhibitors for COVID-19 3CLprotease. The three compounds, Semilicoisoflavone B, Licoflavone B, and Licocoumarin A, displayed a high affinity with the 3CLpro binding pocket of COVID-19. The free energy of binding (FEB) values were 10.91, −10.29, and −10.21 kcal/mole for Autodock 4.2 and −9.81, −9.77, and −9.60 kcal/mole for AutoDockVina, respectively. The three compounds obeyed Lipinski's rule of five, with a little violation in one parameter for two compounds compared to the coordinated ligand N3, which violated more than two rules. The obtained results showed that the compounds interacted with the catalytic dyad (Cys145 and His41) in the binding pocket in the COVID-19 main protease, similar to the coordinated ligand N3. To confirm this finding, experimental studies (in vitro and in vivo) are needed to study the interactions between these com-

pounds and COVID-19.

ACKNOWLEDGEMENT

The authors wish to acknowledge the Faculty of Sciences and Faculty of Health Sciences, Sirte University, for supporting this research.

REFERENCES

Abdusalam, A. A. A., & Murugaiyah, V. (2020). Identification of potential inhibitors of 3CL protease of SARS-CoV-2 from ZINC database by molecular docking-based virtual screening. *Frontiers in molecular biosciences, 7*, 419 .

Ahmed Ali Abdusalam, A., & Vikneswaran, M. (2020). Novel Acetylcholinesterase Inhibitors Identified from ZINC Database Using Docking‐Based Virtual Screening for Alzheimer's Disease. *ChemistrySelect, 5*(12), 3593-3599 .

Asrani, P., Afzal Hussain, K. N., AlAjmi, M. F., Amir, S., Sohal ،S. S., & Hassan, M. I. (2021). Guidelines and safety considerations in the laboratory diagnosis of SARS-CoV-2 infection: a prerequisite study for health professionals. *Risk management and healthcare policy, 14*, 379 .

Burley, S. K., Berman, H. M., Kleywegt, G. J., Markley, J. L., Nakamura, H., & Velankar, S. (2017). Protein Data Bank (PDB): the single global macromolecular structure archive. *Protein Crystallography*, 627-641 .

Chan, J., Azhar, E., Hui, D., & Yuen, K. (2016). Coronaviruses: drug discovery and therapeutic options. *Nat Rev Drug Discov, 15*(5), 327-347 .

Chan, J. F.-W., Kok, K.-H., Zhu, Z., Chu, H., To, K. K.-W., Yuan, S., & Yuen, K.-Y. (2020). Genomic characterization of the 2019 novel human-pathogenic coronavirus isolated from a patient with atypical pneumonia after visiting Wuhan. *Emerging microbes & infections, 9*(1), 221-236 .

Cinatl, J., Morgenstern, B., Bauer, G., Chandra, P., Rabenau, H., & Doerr, H. (2003). Glycyrrhizin, an active component of liquorice roots, and replication of SARS-associated coronavirus. *The lancet, 361*(9374), 2045-2046 .

De Wit, E., Van Doremalen, N., Falzarano, D., & Munster, V. J. (2016). SARS and MERS: recent insights into emerging coronaviruses. *Nature Reviews Microbiology, 14*(8), 523-534 .

Forli, S., Huey ،R., Pique, M. E., Sanner, M. F., Goodsell, D. S., & Olson, A. J. (2016). Computational protein–ligand docking and virtual drug screening with the AutoDock suite. *Nature protocols, 11*(5), 905-919 .

Gills, J. J., LoPiccolo, J., Tsurutani, J., Shoemaker ،R. H., Best, C. J., Abu-Asab, M. S., Borojerdi, J., Warfel, N. A., Gardner, E. R., & Danish, M. (2007). Nelfinavir, A lead HIV protease inhibitor, is a broad-spectrum, anticancer agent that induces endoplasmic reticulum stress, autophagy, and apoptosis in vitro and in vivo. *Clinical Cancer Research, 13*(17), 5183-5194 .

Hariyono, P., Patramurti, C., Candrasari, D. S., & Hariono, M. (2021). An integrated virtual screening of compounds from Carica papaya leaves against multiple protein targets of SARS-Coronavirus-2. *Results in chemistry, 3*, 100113 .

Jacq, N., Breton, V., Chen, H.-Y., Ho, L.-Y., Hofmann, M., Kasam, V., Lee, H.-C., Legré, Y., Lin, S. C., & Maaß, A. (2007). Virtual screening on large scale

grids. *Parallel Computing, 33*(4-5), 289-301 .

Laskowski, R. A., & Swindells, M. B. (2011). LigPlot+: multiple ligand–protein interaction diagrams for drug discovery: ACS Publications.

Lavecchia, A., & Di Giovanni, C. (2013). Virtual screening strategies in drug discovery: a critical review. *Current medicinal chemistry, 20*(23), 2839-2860 .

Makeneni, S., Thieker, D. F & ،.Woods, R. J. (2018). Applying pose clustering and MD simulations to eliminate false positives in molecular docking. *Journal of chemical information and modeling, 58*(3), 605-614 .

Marcelin, A.-G., Lamotte, C., Delaugerre, C., Ktorza, N., Ait Mohand, H ،.Cacace, R., Bonmarchand, M., Wirden, M., Simon, A., & Bossi, P. (2003). Genotypic inhibitory quotient as predictor of virological response to ritonavir-amprenavir in human immunodeficiency virus type 1 protease inhibitor-experienced patients. *Antimicrobial agents and chemotherapy, 47*(2), 594-600 .

McInnes, C. (2007). Virtual screening strategies in drug discovery. *Current opinion in chemical biology, 11*(5), 494-502 .

Morris, G. M., Goodsell, D. S., Halliday, R. S., Huey, R., Hart, W. E., Belew, R. K & ،. Olson, A. J. (1998). Automated docking using a Lamarckian genetic algorithm and an empirical binding free energy function. *Journal of computational chemistry, 19*(14), 1639-1662 .

Pal, M., Berhanu, G., Desalegn, C., & Kandi, V. (2020). Severe acute respiratory syndrome coronavirus-2 (SARS-CoV-2): an update. *Cureus, 12*(3 .(

Pastorino, G., Cornara, L., Soares, S., Rodrigues, F., & Oliveira, M. B. P. (2018). Liquorice (Glycyrrhiza glabra): A phytochemical and pharmacological review. *Phytotherapy research* ،(12)32 ، .2339-2323

Phan, T. (2020). Novel coronavirus: From discovery to clinical diagnostics. *Infection, Genetics and Evolution, 79*, 104211 .

Pompei, R., Pani, A., Flore, O., Marcialis, M., & Loddo, B. (1980). Antiviral activity of glycyrrhizic acid .*Experientia, 36*(3), 304-304 .

Sáez-Llorens, X., Violari, A., Deetz, C. O., Rode, R. A., Gomez, P., Handelsman, E., Pelton, S., Ramilo, O., Cahn, P., & Chadwick, E. (2003). Forty-eight-week evaluation of lopinavir/ritonavir, a new protease inhibitor, in human immunodeficiency virus-infected children. *The Pediatric infectious disease journal, 22*(3), 216-223 .

Sharma, V., Katiyar, A., & Agrawal, R. (2018). Glycyrrhiza glabra: chemistry and pharmacological activity. *Sweeteners*, 87 .

Sliwoski, G., Kothiwale, S., Meiler, J., & Lowe, E. W. (2014). Computational methods in drug discovery. *Pharmacological reviews, 66*(1), 334-395 .

Smith, D. M., Daniel, K. G., Wang, Z., Guida, W. C., Chan, T. H., & Dou, Q. P. (2004). Docking studies and model development of tea polyphenol proteasome inhibitors: applications to rational drug design. *Proteins: Structure, Function, and Bioinformatics, 54*(1), 58-70 .

Stoermer, M. (2020). Homology models of coronavirus 3CLpro protease .

Trott, O., & Olson, A. J. (2010). AutoDock Vina: improving the speed and accuracy of docking with a new scoring function, efficient optimization, and multithreading. *Journal of computational chemistry, 31*(2), 455-461 .

Wang, L., Yang, R., Yuan, B., Liu, Y., & Liu, C. (2015). The antiviral and antimicrobial activities of licorice, a widely-used Chinese herb. *Acta pharmaceutica sinica B, 5*(4), 310-315 .

Yang, X., Yu, Y., Xu, J., Shu, H., Liu, H., Wu, Y., Zhang, L., Yu, Z., Fang, M., & Yu, T. (2020). Clinical course and outcomes of critically ill patients with SARS-CoV-2 pneumonia in Wuhan, China: a single-centered, retrospective, observational study. *The Lancet Respiratory Medicine, 8*(5), 475-481 .

Zehra, Z., Luthra, M., Siddiqui, S. M., Shamsi, A., Gaur, N. A., & Islam, A. (2020). Corona virus versus existence of human on the earth: A computational and biophysical approach. *International Journal of Biological Macromolecules, 161*, 271-281 .

Zoete, V., Grosdidier, A., & Michielin, O. (2009). Docking, virtual high throughput screening and in silico fragment‐based drug design. *Journal of cellular and molecular medicine, 13*(2), 238-248.

تحديد المركبات الطبيعية النشطة بيولوجيا من نبات *Glycyrrhiza glabra* كمثبطات للبروتييز الرئيسي لسارس-كوفيد-2 باستخدام النهج *In-silico*

أشرف أحمد علي عبدالسلام*[1]، غزالة محمد بن هندر[2]

[1] قسم العلوم الصيدلانية، كلية العلوم الصحية، جامعة سرت، ليبيا

[2] قسم الكيمياء، كلية العلوم، جامعة سرت، ليبيا

تاريخ الاستلام: 20 مارس 2022 / تاريخ القبول: 04 يونيو 2022

Doi: https://doi.org/10.54172/mjsc.v37i2.679

المستخلص : تسبب فيروس سارس-كورونا-2 في انتشار جائحة كوفيد-19 وتم الاعلان عنها في بداية سنة 2020 مما تسبب في حالة طوارئ صحية عالمية. حتى الآن، لا توجد أدوية أو لقاحات متاحة ومعتمدة، وهناك حاجة ملحة لاستكشاف وتطوير علاجات جديدة فعالة ضد فيروس كورونا المستجد. بالإضافة إلى ذلك، يعتبر البروتياز الرئيسي لفيروس كورونا المستجد ضروريًا في انتشار تكاثر الفيروس ويعتبر هدفًا لاكتشاف الدواء. لذلك، تعتبر المركبات المشتقة من النباتات مصدرًا مهمًا وقيِّمًا للأدوية الجديدة. تشير هذه الدراسة إلى فحص افتراضي قائم على الإرساء الجزيئي لـ 20 مركبًا تم تحديدها من نبات Glycyrrhiza glabra للبحث عن مركبات قوية ضد البروتييز الرئيسي. أظهرت نتائج الفحص أن المركبات المحددة Semilicoisoflavone B و Licoflavone B و Licocoumarin A أظهرت طاقة ترابط منخفضة كانت 10.91 و10.29- و 10.21- كيلو كالوري / مول لـ AutoDock 4.2 و 9.81- و9.77- و9.60- كيلو كالوري / مول، لـ AutoDock Vina على التوالي. كانت النتائج التي تم الحصول عليها من اقل طاقة ترابط في هذه الدراسة أفضل من المركب المرتبط بالبروتين N3 والذي كان طاقته 7.4- كيلو كالوري / مول. أظهرت المركبات الثلاثة المحتملة تفاعلات مختلفة ومستقرة مع الأحماض الأمينية الأساسية، وخاصة الصباغ التحفيزي (سيستين145، هستادين 41) في جيب الربط للبروتييز الرئيسي. في الختام، تم تحديد ثلاثة مثبطات محتملة بنجاح من نبات *Glycyrrhiza glabra* باستخدام الالتحام الجزيئي والفحص الافتراضي؛ امتثلت هذه المركبات لقاعدة لبنسكي 5 مع انتهاك بسيط وأظهرت انخفاض فى طاقة الترابط وتفاعلات جيدة مع البروتييز الرئيسي. قد تكون هذه المركبات المحددة بمثابة مؤشرات محتملة تساعد في تطوير عوامل علاجية ضد فيروس كورونا المستجد. يوصى بإجراء مزيد من البحث (في المختبر وفي الجسم الحي) للتحقق من النتائج المذكورة أعلاه.

الكلمات المفتاحية : فحص افتراضي، إرساء، *Glycyrrhiza glabra*، كوفيد-19، سارس-كوفيد-2، البروتييز الرئيسي.

*[1] أشرف أحمد علي عبدالسلام: aalmansory@su.edu.ly.، قسم العلوم الصيدلانية، كلية العلوم الصحية، جامعة سرت، ليبيا